PHYSICAL REVIEW B **80**, 081415(R) (2009)

Phonon spectroscopy through the electronic density of states in graphene

E. J. Nicol[1] and J. P. Carbotte[2,3]
[1]*Department of Physics, University of Guelph, Guelph, Ontario, Canada N1G 2W1*
[2]*Department of Physics and Astronomy, McMaster University, Hamilton, Ontario, Canada L8S 4M1*
[3]*The Canadian Institute for Advanced Research, Toronto, Ontario, Canada M5G 1Z8*
(Received 4 August 2009; published 31 August 2009)

In contrast to the normal state of conventional metals for which phonon renormalizations drop out of the electronic density of states, we demonstrate that they remain in the case of graphene and their signature is large and measurable. Furthermore, the electron-phonon interaction, which is fixed in conventional metals, can be tuned over a significant range in graphene by changing the gate voltage. Indeed, a factor of 2 in magnitude should be easily achievable. These two features allow for a normal-state spectroscopy for examining many-body interactions, such as the electron-phonon interaction. We present a procedure to trace the magnitude of the amplitude of the predicted phonon structures which will increase significantly with increasing doping. We also find that the Dirac point zero in the electronic density of states can be lifted and will become quadratic signifying the presence of many-body renormalizations in graphene.

DOI: 10.1103/PhysRevB.80.081415 PACS number(s): 73.20.At, 63.20.kd, 71.38.Cn, 73.40.Gk

It is a remarkable result of many-body physics that in electronic systems in which the density of states (DOS) is constant on the scale of a phonon energy, electron-phonon renormalizations entirely drop out,[1,2] and no phonon signatures are expected or seen. This has now changed with the advent of graphene. Graphene was isolated only in 2004 (Refs. 3 and 4) but has since been extensively studied and found to exhibit many unusual properties. These include a quantum Hall effect, a minimum conductivity, a Berry phase of π and other effects related to the chirality of its charge carriers.[5–7]

In this Rapid Communication, we show how measurements of the DOS in graphene offer an opportunity to obtain detailed information on electron-phonon coupling in sharp contrast to the case of ordinary metals. This is important as it illustrates a strong violation of a well-established result of many-body physics and provides unusual doping-dependent predictions for the manifestation of the electron-phonon interaction in experiments on graphene. This result arises for two reasons. First, the charge carriers exhibit relativistic dispersions with quasiparticle energy ($\epsilon_{\mathbf{k}}$) linear, rather than quadratic, in momentum ($\mathbf{k}$), $\epsilon_{\mathbf{k}}=\pm\hbar v_0|\mathbf{k}|$. Here, v_0 plays the role of the velocity of light and the $\pm$ gives the upper and lower Dirac cones, respectively. At neutrality, the lower cone is fully occupied and the upper one is empty. This dispersion gives rise to an energy dependence of the DOS which is linear. Second, both theory and experiment indicate that the major coupling is to high-energy phonons of order 200 meV.[8–10] Thus, an electron scattering from an initial state to a final state through the assistance of a phonon will sample changes in the DOS on the scale of the phonon energy, which is significant in graphene. Another special feature is that the number of charge carriers can be changed through charging in a field effect device where the chemical potential (μ_0), measured with respect to the Dirac point (neutrality point), is proportional to the square root of the gate voltage. These characteristics offer a rich spectroscopy for the study of phonon effects including their variation in μ_0. By contrast, in conventional metals the electron-phonon interaction is fixed in magnitude.

The graphene renormalized DOS $N(\omega)$ is given by[11–14]

$$\frac{N(\omega)}{N_0}=\int_{-W_C}^{W_C}d\epsilon\frac{|\epsilon|}{\pi}\frac{-\mathrm{Im}\,\Sigma(\omega)}{[\omega-\mathrm{Re}\,\Sigma(\omega)+\mu-\epsilon]^2+[\mathrm{Im}\,\Sigma(\omega)]^2}, \tag{1}$$

with $N_0=2/\pi\hbar^2v_0^2$. In Eq. (1), W_C is an upper cutoff on the Dirac cones given by $\sqrt{\pi\sqrt{3}}t$, with t as the nearest-neighbor hopping parameter, and $\Sigma(\omega)$ is the electronic self-energy given by[12]

$$\Sigma(\omega)=\int_0^{+\infty}d\nu\alpha^2F(\nu)\int_{-\infty}^{+\infty}d\omega'\frac{N(\omega')}{N_0W_C}\times\left[\frac{n(\nu)+f(-\omega')}{\omega-\omega'-\nu+i0^+}+\frac{n(\nu)+f(\omega')}{\omega-\omega'+\nu+i0^+}\right], \tag{2}$$

where $\alpha^2F(\nu)$ is the electron-phonon spectral density and $n(\nu)$ and $f(\omega')$ are, respectively, the Bose-Einstein and Fermi-Dirac distribution functions at temperature T. For the bare band case [$\Sigma(\omega)\to 0$], the chemical potential μ reduces to its noninteracting value μ_0 and sets the doping level. Also, the Lorentzian form in Eq. (1) reduces to $\delta(\omega+\mu_0-\epsilon)$ and the DOS becomes $|\omega+\mu_0|$.

Park *et al.*[8] performed a full first-principles study of the electron-phonon interaction in graphene and found that the result could be approximated by an Einstein mode at 200 meV. In this case, the electronic self-energy, at zero temperature, is given by an analytic form with[15]

$$\mathrm{Re}\,\Sigma(\omega)=\frac{A}{W_C}\left\{\omega_E\ln\left|\frac{(\mu_0+\omega+\omega_E)^2}{(\omega^2-\omega_E^2)}\right|-(\mu_0+\omega)\ln\left|\frac{W_C^2(\omega+\omega_E)}{(\omega-\omega_E)(\omega+\mu_0+\omega_E)^2}\right|\right\}, \tag{3}$$

where A is the area under the Einstein mode and ω_E its frequency. For simplicity, we have assumed in writing Eq. (3) that W_C is larger than any other energy of interest, but in

all numerical results presented here, this approximation was not made. The corresponding imaginary part is $-\mathrm{Im}\,\Sigma(\omega) = \frac{\pi A}{W_C}|\omega-\omega_E+\mu_0|$, for $\omega_E<\omega<W_C-\mu_0+\omega_E$ and $\frac{\pi A}{W_C}|\omega+\omega_E+\mu_0|$ for $-\omega_E>\omega>-W_C-\mu_0-\omega_E$. In terms of this self-energy, the renormalized density of states is given by

$$\frac{N(\omega)}{N_0} = \frac{\tilde{\omega}}{\pi}\left[2\tan^{-1}\left(\frac{\tilde{\omega}}{\Gamma}\right) - \tan^{-1}\left(\frac{\tilde{\omega}-W_C}{\Gamma}\right) - \tan^{-1}\left(\frac{\tilde{\omega}+W_C}{\Gamma}\right)\right] + \frac{\Gamma}{2\pi}\ln\left\{\frac{[(\tilde{\omega}-W_C)^2+\Gamma^2][(\tilde{\omega}+W_C)^2+\Gamma^2]}{(\tilde{\omega}^2+\Gamma^2)^2}\right\}, \tag{4}$$

where $\Gamma=-\mathrm{Im}\,\Sigma(\omega)$ and $\tilde{\omega}=\omega-\mathrm{Re}\,\Sigma(\omega)+\mu$. For finite μ, the problem no longer has particle-hole symmetry and $\mathrm{Re}\,\Sigma(\omega=0)$ is not zero and provides a shift in chemical potential from bare to dressed value with $\mu=\mu_0+\mathrm{Re}\,\Sigma(\omega=0)$.[13,16] For a clean system Γ will vanish for $-\omega_E<\omega<\omega_E$, and Eq. (4) reduces to

$$\frac{N(\omega)}{N_0} = \tilde{\omega}\ \mathrm{sgn}\ \tilde{\omega}, \quad \text{for} \quad -\omega_E<\omega<\omega_E. \tag{5}$$

In this special range, the DOS is very closely related to the $\mathrm{Re}\,\Sigma(\omega)$. Returning to Eq. (1), it is important to realize that, for infinite bands with constant DOS, the $|\epsilon|$ factor would not appear and the integral over ϵ would give a constant independent of ω so that phonon renormalizations simply drop out. Graphene is very different.

While Eq. (3) has been written for a single Einstein oscillator, it nevertheless provides us with valuable insight into the relationship between phonon structure and the real part of the self-energy. $\mathrm{Re}\,\Sigma(\omega)$ has singularities of the form $\ln|\omega\pm\omega_E|$ at $\omega=\pm\omega_E$ and a third weaker logarithmic singularity of the type $(\omega+\omega_E+\mu_0)\ln|\mu_0+\omega+\omega_E|$ at $\omega=-(\mu_0+\omega_E)$. The neutrality point is special, however. For $\mu_0=0$, only two singularities remain and they are both of the weaker kind $(\omega\pm\omega_E)\ln|\omega\pm\omega_E|$. In a real system there will of course be a distribution of phonons and the self-energy of Eq. (3) needs to be averaged over such a distribution. This will reduce the prominence of the expected singularities in this quantity. In such a case it becomes useful to consider a first derivative $-d\,\mathrm{Re}\,\Sigma(\omega)/d\omega$. This is shown in Fig. 1 for four values of the chemical potential, $\mu_0=0$, 150, 500, and 700 meV. The phonon distribution used in these numerical calculations was a truncated Lorentzian centered on $\omega_E=200$ meV with width $\delta=15$ meV.[12,17] As expected the top left frame exhibits only two phonon anomalies while the three other frames have three. Also in these three cases the anomalies at $\omega=\pm\omega_E$ are much more pronounced than the ones at $\omega=-(\omega_E+\mu_0)$ and also than those in the top left frame. In all four frames, the black dotted horizontal line was drawn through the local minimum at $\omega=0$ and identifies the value of the electron-phonon mass renormalization parameter λ as we will now describe. For ω small near the Fermi energy ($\omega=0$), $\mathrm{Re}\,\Sigma(\omega)$ in Eq. (3) can be shown to vary as $\mathrm{Re}\,\Sigma(\omega)\simeq-\lambda\omega+\mathrm{Re}\,\Sigma(\omega=0)$ and the dressed quasiparticle

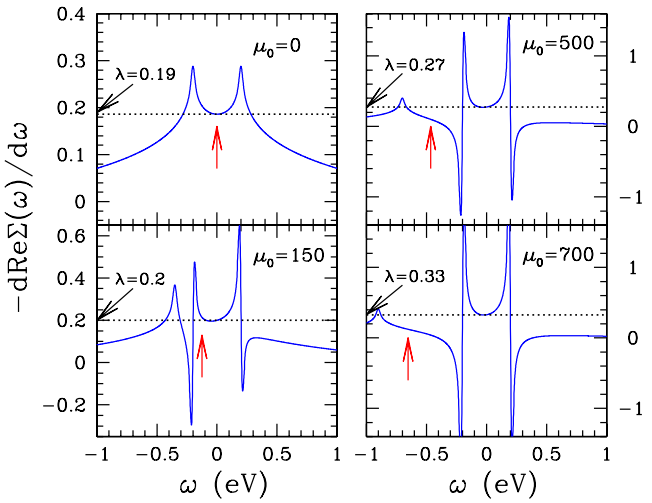

FIG. 1. (Color online) $-d\,\mathrm{Re}\,\Sigma(\omega)/d\omega$ vs ω for a truncated Lorentzian electron-phonon spectral density peaked around 200 meV. Curves are for $\mu_0=0$, 150, 500, and 700 meV.

energy $E_{\mathbf{k}}$ is given by the equation $E_{\mathbf{k}}-\mathrm{Re}\,\Sigma(E_{\mathbf{k}})+\mu = \pm\hbar v_0|\mathbf{k}|=E_{\mathbf{k}}(1+\lambda)+\mu_0$. Or $E_{\mathbf{k}}=[\pm\hbar v_0|\mathbf{k}|-\mu_0]/(1+\lambda) = \pm\hbar v_0(k-k_F)/(1+\lambda)$, which means that λ simply renormalizes the bare Fermi velocity from v_0 to $v_0^*\equiv v_0/(1+\lambda)$. As Fig. 1 shows, λ grows with increasing μ_0 as Eq. (3) implies. The red vertical arrow indicates the Dirac point defined by $|\mathbf{k}|=0$.

The relationship between boson structure in the self-energy and its manifestation in the DOS is given by Eq. (4). Results for $N(\omega)$ are shown in Fig. 2. The frame (a) is for $\mu_0=150$ meV, which is smaller than ω_E and (b) is for $\mu_0=500$ meV $>\omega_E$. The shaded yellow region is the occupied part of the bare band which is shown as the black dotted curve. Phonon renormalizations change the shape of the DOS and hence the value of the chemical potential must be altered to keep the correct number of particles. The long black and short blue arrows point to the value of the bare and dressed chemical potential with $\mu-\mu_0=\mathrm{Re}\,\Sigma(\omega=0)$. Phonon anomalies are clearly seen in the dressed curves. To emphasize this structure an Einstein spectrum was used with $\omega_E=200$ meV so that the phonon structures fall at $\omega=\pm\omega_E$,

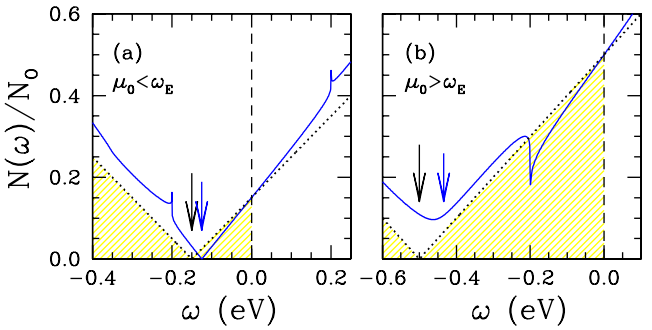

FIG. 2. (Color online) (a) $N(\omega)/N_0$ (in eV) vs ω for the bare chemical potential $\mu_0=150$ meV. The solid curve gives the phonon renormalized case and the dotted gives the bare band case. The arrows show the bare (long) and renormalized (short) value of μ. (b) Same as for (a) but with $\mu_0=500$ meV.

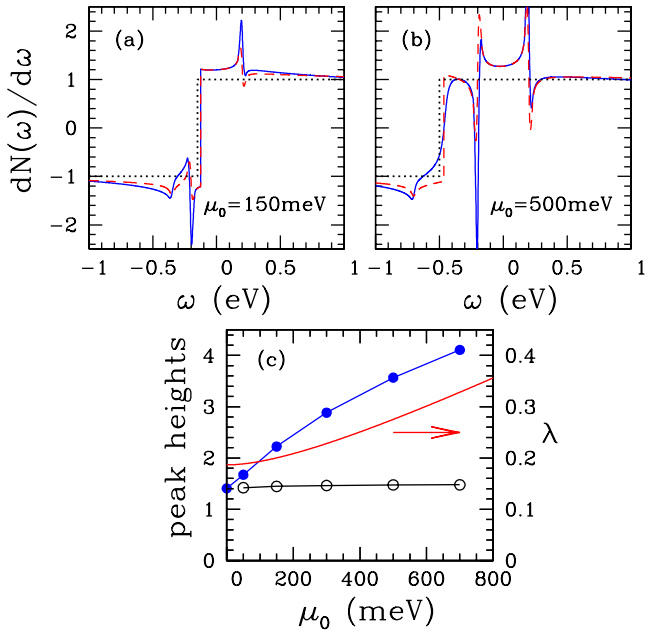

FIG. 3. (Color online) (a) $dN(\omega)/d\omega$ vs ω (solid curve) for $\mu_0=150$ meV. The dotted curve sets a baseline and is the bare band case. The dashed, which is for comparison, is $[1-d\,\mathrm{Re}\,\Sigma(\omega)/d\omega]\mathrm{sgn}(\omega+\omega_d)$. (b) Same as for (a) but with $\mu_0=500$ meV. (c) The absolute height of the phonon peaks at about $\omega=\omega_E$ (solid dots) and $-(\mu_0+\omega_E)$ (open circles) along with the λ variation in μ_0, the latter indicated as the red solid curve using the right-hand axis (indicated by the arrow).

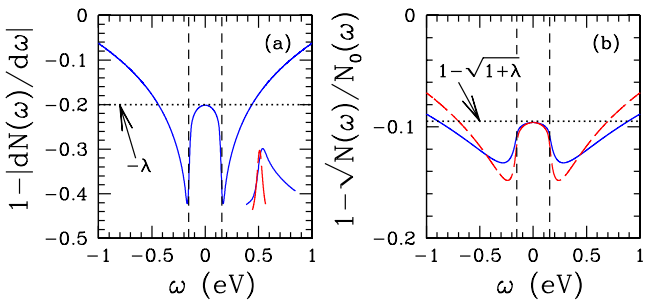

FIG. 4. (Color online) (a) $1-|dN(\omega)/d\omega|$ vs ω for $\mu_0=0$ and $\omega_E=155$ meV (solid blue curve). The inset on the lower right compares the phonon region with the input electron-phonon spectral density (red-dashed curve). (b) $1-\sqrt{N(\omega)/N_0(\omega)}$ vs ω (solid blue curve) compared with the result using the procedure of Li *et al.* (long-dashed red curve).

one on either side of the Fermi energy. The expected singularity at $\omega=-(\omega_E+\mu_0)$ is by comparison very weak and appears as a slight change in slope in Fig. 2. Two additional features of these curves are to be noted. At the Fermi energy ($\omega=0$), the dressed and bare DOS have exactly the same value. In the region of the Fermi energy Eq. (5) applies and $N(\omega)/N_0=|\omega(1+\lambda)+\mu_0|$, which differs from its bare value only by the additional factor of $(1+\lambda)$. At $\omega=0$, this difference disappears and dressed and bare DOS are the same. Phonons do not change the value of the DOS at the Fermi level. The slope out of $\omega=0$, however, is changed by a factor of $(1+\lambda)$ as can be seen in both frames of Fig. 2, and we also note that this linear behavior persists over a considerable energy range set by the value of the Einstein oscillator. Recognizing that the normalization for the DOS is $N_0\sim 1/v_0^2$, one might naively think that the $(1+\lambda)$ renormalization can be included in $N(\omega)$ simply by changing v_0 to v_0^* in N_0, but we see here that this is not correct. Only one $(1+\lambda)$ factor enters and not its square. The basic reason underlying this fact is that the coherent part of the electronic Green's function, which defines the quasiparticles in the interacting system, contains only $1/(1+\lambda)$ of the spectral weight. The remainder $\lambda/(1+\lambda)$ is found in the incoherent piece describing phonon-assisted processes.

Phonon structure in $N(\omega)$ can be brought out through differentiation. Results for $dN(\omega)/d\omega$ vs ω are given in Fig. 3 as the solid blue curves, where $N(\omega)$ is normalized by N_0. Frame (a) is for $\mu_0=150$ meV and (b) is for 500 meV. The vertical drop where $dN(\omega)/d\omega$ goes from positive to negative is at the Dirac point of the interacting system. Comparison with the bare band case, the dotted black line, shows a small shift of the position of the Dirac point between bare and dressed case. The bare case provides a useful reference line about which the effects of the electron-phonon interaction are easily seen. Besides the phonon structures at $\omega=\pm\omega_E,-(\omega_E+\mu_0)$, we note that the height of the curve above one at $\omega=0$ gives the value of λ directly which increases significantly with increasing value of chemical potential [as shown by the red solid curve in (c)]. The red dashed line is included for comparison and gives $-d\,\mathrm{Re}\,\Sigma(\omega)/d\omega$. There are some differences between these two sets of results but we can conclude that all qualitative features seen in the DOS curves can be seen in the $\mathrm{Re}\,\Sigma(\omega)$. This is not to say that the imaginary part of $\Sigma(\omega)$ plays no significant role. In frame (b), we see clearly that the jump at the Dirac point energy is no longer vertical but exhibits some smearing. This can be traced to the behavior about the Dirac point in the DOS shown in Fig. 2(b). The DOS no longer goes to zero at this point (ω_d) but rather has a minimum about which it rises as a quadratic $(\omega-\omega_d)^2$, seen in experiment.[18] We can show that for $|(\omega-\omega_d)Z|\ll\Gamma$,

$$\frac{N(\omega)}{N_0}=\frac{2\Gamma}{\pi}\ln\left|\frac{W_C}{\Gamma}\right|+\frac{(\omega-\omega_d)^2Z^2}{\pi\Gamma},\tag{6}$$

with $Z\equiv 1-[d\,\mathrm{Re}\,\Sigma(\omega)/d\omega]_{\omega=\omega_d}$ and $\Gamma\equiv-[\mathrm{Im}\,\Sigma(\omega)]_{\omega=\omega_d}$, which shows the lifting of the Dirac point and its conversion from linear to quadratic in $(\omega-\omega_d)$. This immediately leads to the smearing at the Dirac point noted in the blue curve of Fig. 3(b). In Fig. 3(c), we plot the absolute value of the height of the phonon structures as a function of μ_0 for the $\alpha^2F(\nu)$ spectrum used here, a truncated Lorentzian (see in the inset of Fig. 4, long-dashed red curve). While the height of the phonon peak at $\omega=-(\omega_E+\mu_0)$ hardly changes with doping (μ_0) the other two peaks do, note the curve for $\omega=\omega_E$. We have not plotted the peak height for $\omega=-\omega_E$ as for $\mu_0<\omega_E$ it is similar to the result for $\omega=\omega_E$ and for $\mu_0>\omega_E$ it becomes ambiguous. These predictions provide verifiable tests that observed structures are indeed due to phonons. They also show how the increase in the DOS at the

Fermi surface with increasing doping is reflected in larger coupling to the phonons.

In Fig. 4(a), we show results for $[1-|dN(\omega)/d\omega|]$ in the specific case of $\mu_0=0$ which is close to the case recently observed in the scanning tunneling miscroscopy (STM) results of Li *et al.*[9] To conform with those experiments, we have used $\omega_E=155$ meV, with $\omega=\pm\omega_E$ shown as the vertical black dashed lines. The horizontal black dotted line through the local maximum of the solid blue curve at $\omega=0$ identifies the value of λ which we took to be 0.2. A second important feature is the phonon structure which reflects the underlying $\alpha^2F(\nu)$ spectrum used. It is shown in the inset as the long-dashed red curve where it is scaled down and compared with the absolute value of the blue curve about $\omega=155$ meV. While there is some agreement, the two curves have different profiles with the blue solid one much broader than the red long-dashed one. It is clear that such a plot is very useful in identifying phonon structure, i.e., not just the value of the mass enhancement factor λ involved but also the position of the peaks in $\alpha^2F(\nu)$ and their strength. In experiments, it may be more desirable not to differentiate. In Fig. 4(b), we show as the solid blue curve a different quantity $1-\sqrt{N(\omega)/N_0(\omega)}$, where $N_0(\omega)$ is the bare band density of states. In this quantity, the value of the local maximum at $\omega=0$ gives $1-\sqrt{1+\lambda}=-0.095$ rather than the $-\lambda$ of frame (a). We also note that the phonon structures at $\omega=\pm\omega_E$ are not as sharp, however, some signature of a sharp peak in the $\alpha^2F(\nu)$ used remains. The long-dashed red curve is for comparison and represents the quantity that was used by Li *et al.*[9] in their analysis of their STM data. They use a definition of an effective Fermi velocity dependent on E based on an integration of their conductance. They define $v_F^{\mathrm{eff}}=dE/\hbar dk$ with $k=\pm\left|\int_{\omega_d}^{E}N(\omega)d\omega\right|^{1/2}$, where ω_d is the energy locating the Dirac point. Like the blue solid curve, the maximum at $\omega=0$ provides $1-\sqrt{1+\lambda}$ and the phonon structures at $\omega=\pm\omega_E$ are clearly seen. The Li *et al.*[9] estimate of $\lambda=0.26$ is close to the 0.3 value from angle-resolved photoemission experiments.[10] Our own estimate based on the STM data is somewhat higher but carries considerable uncertainty because of the experimental noise. An important point to note between Figs. 4(a) and 4(b) is to reiterate that the many-body renormalizations correct $N(\omega)$ by a $(1+\lambda)$ factor. Assuming $|\epsilon|/v_F^2\rightarrow|\epsilon|/v_F^{*2}$ would over estimate the correction by an additional factor of $(1+\lambda)$.

In contrast to the standard expectation in wideband metals with nearly constant DOS on the phonon energy scale, phonon structure does appear prominently in the DOS of graphene and this can be used as a spectroscopy for determining electron-phonon coupling. The mass enhancement parameter λ can be extracted directly from the data around the Fermi energy and three prominent peaks can be identified at $\omega=\pm\omega_E$ and $\omega=-(\omega_E+\mu_0)$ associated with each Einstein mode. The size of these additional structures increases with increasing doping as does the mass enhancement λ, reflecting the increase in the underlying DOS. Indeed, due to the linear DOS, the electron-phonon interaction can be tuned over a significant range of values simply by changing the applied gate voltage in a field effect device. The presence of many-body renormalizations is also signaled by the lifting of the Dirac point zero in the DOS. With these features, graphene provides a rich laboratory in which to study induced variations in many-body renormalizations.

We thank S. Sharapov for valuable assistance and insight, and E. Andrei and G. Li for discussion about their work. Support was provided by NSERC and CIFAR.

[1] G. Grimvall, *The Electron-Phonon Interaction in Metals* (North-Holland, New York, 1981).
[2] R. E. Prange and L. P. Kadanoff, Phys. Rev. **134**, A566 (1964).
[3] K. S. Novoselov, A. K. Geim, S. V. Morozov, D. Jiang, Y. Zhang, S. V. Dubonov, I. V. Grigorieva, and A. A. Firsov, Science **306**, 666 (2004).
[4] K. S. Novoselov, D. Jiang, F. Schedin, T. J. Booth, V. V. Khotkevich, S. V. Morozov, and A. K. Geim, Proc. Natl. Acad. Sci. U.S.A. **102**, 10451 (2005).
[5] K. S. Novoselov, A. K. Geim, S. V. Morozov, D. Jiang, M. I. Katsnelson, I. V. Grigorieva, S. V. Dubonov, and A. A. Firsov, Nature (London) **438**, 197 (2005).
[6] Y. Zhang, Y. W. Tan, H. L. Stormer, and P. Kim, Nature (London) **438**, 201 (2005).
[7] A. K. Geim and K. S. Novoselov, Nature Mater. **6**, 183 (2007).
[8] C. H. Park, F. Giustino, M. L. Cohen, and S. G. Louie, Phys. Rev. Lett. **99**, 086804 (2007).
[9] G. Li, A. Luican, and E. Y. Andrei, Phys. Rev. Lett. **102**, 176804 (2009); also see arXiv:0803.4016v1.
[10] A. Bostwick, T. Ohta, T. Seyller, K. Horn, and E. Rotenberg, Nat. Phys. **3**, 36 (2007).
[11] A. Knigavko, J. P. Carbotte, and F. Marsiglio, Europhys. Lett. **71**, 776 (2005).
[12] F. Dogan and F. Marsiglio, Phys. Rev. B **68**, 165102 (2003).
[13] B. Mitrović and J. P. Carbotte, Can. J. Phys. **61**, 758 (1983).
[14] A. Knigavko and J. P. Carbotte, Phys. Rev. B **72**, 035125 (2005).
[15] T. Stauber and N. M. R. Peres, J. Phys.: Condens. Matter **20**, 055002 (2008).
[16] J. M. Luttinger and J. C. Ward, Phys. Rev. **118**, 1417 (1960).
[17] J. P. Carbotte, E. J. Nicol, and S. G. Sharapov, arXiv:0908.2608 (unpublished).
[18] F. Wang, Y. Zhang, C. Tian, C. Girit, A. Zettl, M. Crommie, and Y. R. Shen, Science **320**, 206 (2008).